

# Aeroelastic Effects on the B-2 Maneuver Response

B. A. Winther,\* D. A. Hagemeyer,† R. T. Britt,‡ and W. P. Rodden§  
*Northrop Grumman Corporation, Pico Rivera, California 90660*

Differential sensor rotations relative to the mean inertia axes usually are neglected in simulations of the quasisteady frequency response. For control-configured flying-wing aircraft, however, this aeroelastic effect may be significant as demonstrated by analyses of the U.S. Air Force-Northrop B-2 aircraft. A correction for the axes rotation has been provided by Rodden and Love who formulated the unaugmented vehicle equations in terms of motion variables measured in a structurally restrained system. This article, while retaining the original mean axes formulation, extends the Rodden–Love concept to the sensor output equations, which are required for modeling of aeroservoelastic effects. By applying the modified equations, longitudinal maneuver analyses are performed and correlated with flight test data.

## Nomenclature

$A, B$	= matrices in equations of motion
$C, D$	= matrices in output equations
$C_z, C_m$	= aerodynamic coefficients
$c$	= reference chord length
$d$	= structural deflection derivative
$F$	= generalized external force vector
$G, M$	= matrices in intermediate formulation
$g$	= acceleration of gravity
$h$	= structural displacement
$I$	= pitch moment of inertia
$i$	= $8I/\rho Sc^3$
$l$	= c.g. distance from reference station
$m$	= vehicle mass
$n_z$	= vertical load factor
$q$	= generalized coordinate
$S$	= reference area
$s$	= sensor distance from reference station
$t$	= time
$u$	= state variable vector
$V$	= velocity
$X, Y, Z$	= Earth-fixed coordinates
$x, y, z$	= mean axes coordinates
$\alpha$	= angle of attack
$\gamma$	= flight-path angle
$\Delta$	= prefix indicating offset from initial value
$\delta$	= control deflection
$\varepsilon$	= flexibility increment
$\theta$	= pitch angle
$\lambda$	= $2l/c$
$\mu$	= $2m/\rho Sc$
$\nu$	= $2V^2/gc$
$\rho$	= air density
$\sigma$	= $2s/c$
$\tau$	= $c/2V$
$\psi$	= structural deflection component

## Subscripts

$s$	= structural axes value
$x$	= $\partial(\ )/\partial x$
$0$	= initial value

## Superscripts

$:$	= $d(\ )/dt$
$,$	= mean flight-path axes value

## Introduction

FOR motion simulator applications, the flexible vehicle equations customarily are written in terms of aerodynamic coefficients that are determined with the aeroelastic structure restrained in some statically determinate manner near the c.g. Inertial relief effects for the free-flying aircraft then are taken into account through separate aeroelastic inertial coefficients determined also for the restrained system undergoing translational and rotational accelerations. This formulation offers the advantage that basic aerodynamic characteristics, e.g.,  $C_{za}$ ,  $C_{ma}$ , etc., depend only on Mach number and altitude, but are independent of the weight; while the inertial coefficients, e.g.,  $C_{z\ddot{a}}$ ,  $C_{m\ddot{a}}$ , etc., depend on the weight and its distribution, as well as Mach number and altitude. Although these equations have been implemented rather successfully on simulators for many years, it can be shown that the formulation is inexact in the sense that it does not conserve angular momentum and, as a consequence, yields solutions that for some configurations may vary significantly with the choice of restraint. To correct the deficiency, Rodden and Love<sup>1</sup> established the relationship between the structural axes (at the restraint) and the mean body axes required for conservation of angular momentum. In the case of symmetric motion, it is the angle between the two longitudinal axes that needs to be considered.

Early results of the B-2 flight test program verified the basic aeroelastic stability and flying quality performance. A detailed correlation with analytical simulations indicated, however, that some aerodynamic terms required adjustments, which in some cases were difficult to justify. This anomaly, together with an apparent inconsistency between quasisteady and dynamic analyses, led to a review of the simulator equations that were known to contain several approximations. One approximation that had been made for the sake of simplicity, neglected the relative motion between the mean body axes and the structural reference frame as previously discussed. During the review, it was concluded that, for control-configured flying-wing aircraft like the B-2, the axis rotation is an important component of the aeroelastic response, and a decision was made to revise the simulator equations of motion as well as the associated sensor output equations.

Received May 20, 1993; presented as Paper 93-3664 at the AIAA Atmospheric Flight Mechanics Conference, Monterey, CA, Aug. 9–11, 1993; revision received Sept. 12, 1994; accepted for publication Jan. 15, 1995. Copyright © 1993 by the American Institute of Aeronautics and Astronautics, Inc. All rights reserved.

\*Senior Technical Specialist, Loads and Dynamics, B-2 Division. Associate Fellow AIAA.

†Manager, Flight Control Laws, B-2 Division.

‡Manager, Loads and Dynamics, B-2 Division. Member AIAA.

§Consultant, B-2 Division. Fellow AIAA.

In the analysis of control-configured vehicles, the output equations describe the motion measured by sensors that are used in feedback control of the system. To provide a proper model of the feedback system, the sensor equations must represent the motion on the structure rather than on the mean body axis. This article extends the concepts of Ref. 1 to the quasisteady response equations, paying particular attention to the structural dynamics and accounting for the relative motion of the mean axes. Since the general equations are quite complex, we will limit the discussion to small perturbations about an initial reference condition of steady, symmetric flight. Consequently, the equations are linear in the motion variables. As in Ref. 1, the fore/aft degree of freedom (DOF) is eliminated from consideration by the assumption of constant (unperturbed) forward velocity.

### Unaugmented Aircraft Equations

The equations of motion may be formulated in any one of the following three types of coordinate systems: 1) structural axes ( $x_s, y_s, z_s$ ); 2) mean flight-path axes ( $x', y', z'$ ); and 3) mean body axes ( $x, y, z$ ).

As established in Ref. 1 and discussed in the Introduction, the use of structurally attached axes for the equations of motion [Eq. (22) in Ref. 1] requires an additional relationship [Eq. (35) in Ref. 1] describing the orientation of the mean body axes in terms of structural axes motion variables. This formulation contains aerodynamic coefficients for the restrained structure as well as aeroelastic coefficients that account for inertial relief effects of the free-flying aircraft. Mean flight-path axes, commonly used in structural dynamics, result in a more direct description of aeroelastic deformations. However, since this article is limited to the quasisteady region of the aircraft response, we will use the mean flight-path axes only to introduce the mean body axes system that is the conventional one in flight mechanics. This latter system also is used in an alternate formulation derived for unaugmented aircraft by Dusto and his associates.<sup>2,3</sup>

The mean flight-path axes are aligned with the unperturbed flight path of the aircraft and move with its average (initial) velocity relative to the Earth-fixed system ( $X, Y, Z$ ). Transformations between the two coordinate systems (see Fig. 1) are determined by

$$\begin{cases} X = (x' + V\Delta t)\cos \gamma_0 + z' \sin \gamma_0 \\ Y = y' \\ Z = -(x' + V\Delta t)\sin \gamma_0 + z' \cos \gamma_0 \end{cases} \quad (1)$$

The time increment  $\Delta t$  is measured from the initial reference condition when the aircraft flight-path angle is

$$\gamma_0 = \theta_0 - \alpha_0 \quad (2)$$

With plunge and pitch DOFs represented by generalized coordinates  $q_1$  and  $q_2$ , a displacement of the rigid (i.e., un-loaded) airframe in the  $z'$  direction may be described by

$$h = q_1 - x' q_2 \quad (3)$$

leading to the following equations of motion:

$$\mathbf{F} = \begin{bmatrix} m & -ml \\ -ml & I \end{bmatrix} \begin{Bmatrix} \ddot{q}_1 \\ \ddot{q}_2 \end{Bmatrix} \quad (4)$$

The vector  $\mathbf{F}$  is derived from a combination of aerodynamic and gravitational forces.

As already noted, we will formulate the equations of motion in a body axes system. The  $x$  axis in this type of system may be oriented along any convenient reference line, such as the chordline of the wing root, the principal inertia axis, or an initial wind axis (also named stability axis). Even though the

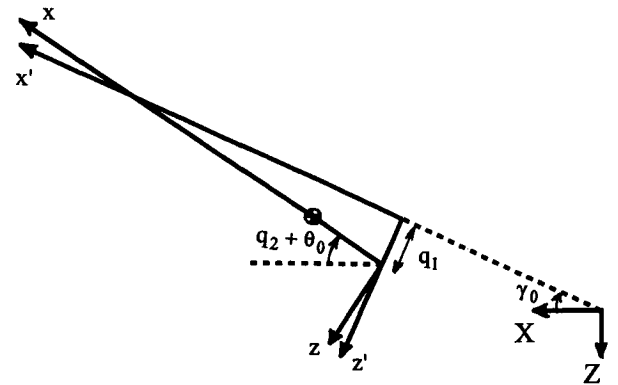


Fig. 1 Illustration of two different mean axes concepts.

orientation may differ from one problem to another (as with the stability axis), the common characteristic of all body axes is that they are fixed relative to the aircraft c.g. In the present discussion we will employ "mean" body axes that are lined up with the instantaneous, average position of the flexing structure, such that the static mass moments about the axes are constant (zero, for  $l = 0$ ) throughout the maneuver. When angular accelerations can be considered independent of the spacial coordinates, as we assume here, the mean axes become parallel (identical, for  $l = 0$ ) to the principal axes.

The generalized coordinates of Eq. (3) may be expressed in terms of conventional body axes variables. One relationship is derived from the linearized boundary condition on the moving wing surface:

$$\alpha(x) - \alpha_0 = \frac{\left( \frac{\partial h}{\partial t} - \frac{V \partial h}{\partial x'} \right)}{V} \quad (5)$$

At the reference station of the mean body axis (i.e.,  $x = 0$ ) we obtain

$$\begin{cases} \Delta \alpha = \dot{q}_1/V + q_2 \\ \dot{\theta} = \dot{q}_2 \end{cases} \quad (6)$$

Other relationships may be derived by observing

$$\begin{cases} \ddot{q}_1 = g(\cos \theta - n_z) \\ q_2 = \theta - \theta_0 \end{cases} \quad (7)$$

Applying the small perturbation linearization and the definitions of stability derivatives from Ref. 4, the equations of motion for level flight (i.e.,  $\gamma_0 = 0$ ) are reduced to the following state vector formulation:

$$\dot{\mathbf{u}} = A\mathbf{u} + B\Delta\delta \quad (8)$$

where

$$\mathbf{u} = \begin{Bmatrix} \Delta \alpha \\ \dot{\theta} \end{Bmatrix}$$

$$A = M^{-1} \begin{bmatrix} C_{z\alpha}/\tau & (C_{zq} + 2\mu) \\ C_{m\alpha}/\tau & (C_{mq} - \mu\lambda) \end{bmatrix}$$

$$B = M^{-1} \begin{Bmatrix} C_{z\delta}/\tau \\ C_{m\delta}/\tau \end{Bmatrix}$$

$$M = \begin{bmatrix} (2\mu - C_{z\alpha}) & -2\mu\lambda\tau \\ -(\mu\lambda + C_{m\alpha}) & i\tau \end{bmatrix}$$

We note that Eq. (8) represents small perturbations about a steady, level, and symmetric flight condition. It describes the maneuver response of the aircraft gravitational center and is formulated in terms of motion variables at the mean axis reference station.

Another important observation is that in the quasisteady frequency range, the equation is valid for elastic airframes as long as the stability derivatives are measured relative to the principal (i.e., mean) axes of the flexing structure. Even though the elastic deformation does not appear explicitly in the basic equations of motion, it needs to be accounted for in simulations involving the sensor response. The sensor equations are derived in the following section with the continued assumption of quasisteady structural equilibrium during the maneuver.

### Sensor Output Equations

For discussion of the output equations, we introduce a coordinate system  $(x_s, y_s, z_s)$  attached to the structure at the sensor location  $(x, y, z) = (s, 0, h_s)$ . In this reference frame, the c.g. moves and the principal axes rotate as the aircraft flexes (see Fig. 2). The  $z$  coordinate  $h_s$  denotes the vertical displacement of the sensor relative to the mean  $x$  axis. If the unaugmented aircraft equations are transformed to structural axes, as described in Ref. 1, the equations of motion will include terms that represent aerodynamic forces generated by the flexibility increment:

$$\varepsilon_s = \alpha_s - \alpha(s) \quad (9)$$

where the angle of attack  $\alpha(s)$  is measured at  $x = s$  in the mean axes system, and  $\alpha_s$  is measured in the structural axes system. In the following, the sensor motions will be expressed in mean axes variables so that the basic aircraft equations are retained as shown in Eq. (8). Using Eq. (5) to derive the angle of attack produced by structural flexing we obtain

$$\varepsilon_s = -h_{sx} + \dot{h}_s/V \quad (10)$$

The quantity  $h_{sx}$  denotes the angular deflection of the sensor relative to the mean axis. Thus, the sensor motions are described by

$$\begin{cases} \alpha_s = \alpha(s) + \varepsilon_s \\ \dot{\theta}_s = \dot{\theta} - \dot{h}_{sx} \end{cases} \quad (11)$$

Aerodynamic forces generated by the time derivative of  $h_s$  in Eq. (10) vanish at the quasisteady limit so that the flexibility increment becomes simply  $\varepsilon_s = -h_{sx}$ . This increment, which is obtained from structural analysis, may be expressed in terms of partial derivatives  $d_i$ . One deflection component  $\psi_1$  is considered caused by aerodynamic loads only, whereas the remaining part  $\psi_2$  is derived from a combination of aerodynamic

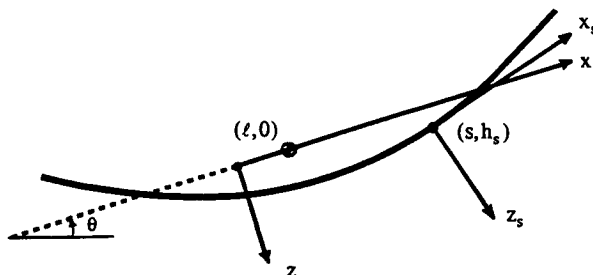


Fig. 2 Illustration of relative motion between structural and mean axes.

and inertial forces. The two components of  $\varepsilon_s$  are written in the following expanded form:

$$\begin{cases} \psi_1 = -(d_0 + d_1\alpha_s + d_2\tau\dot{\alpha}_s + d_3\tau\dot{\theta}_s + d_4\delta) \\ \psi_2 = -[d_5n_z(s) + d_6\tau^2\ddot{\theta}] \end{cases} \quad (12)$$

where  $d_0$  represents the incremental sensor rotation due to aerodynamic loads at zero mean axis incidence. The remaining derivatives, being equivalent to the  $\alpha$  coefficients of Ref. 1 (Eq. 37), are defined as follows:

$$\begin{aligned} d_1 &= \frac{\partial h_{sx}}{\partial \alpha_s} = \alpha_\alpha - 1 \\ d_2 &= \frac{\partial h_{sx}}{\partial (\tau\dot{\alpha}_s)} = \alpha_\alpha \\ d_3 &= \frac{\partial h_{sx}}{\partial (\tau\dot{\theta}_s)} = \alpha_\theta \\ d_4 &= \frac{\partial h_{sx}}{\partial \delta} = \alpha_\delta \\ d_5 &= \frac{\partial h_{sx}}{\partial n_z(s)} = -\alpha_z \\ d_6 &= \frac{\partial h_{sx}}{\partial (\tau^2\ddot{\theta})} = \nu\alpha_\theta \end{aligned} \quad (13)$$

Applying these derivatives in Eq. (11) we obtain

$$\begin{cases} \alpha_s = \frac{[\alpha(s) - d_0 - d_2\tau\dot{\alpha}(s) - d_3\tau\dot{\theta} - d_4\delta - d_5n_z(s) - d_6\tau^2\ddot{\theta}]}{(1 + d_1)} \\ \dot{\theta}_s = \dot{\theta} + \dot{\varepsilon}_s \end{cases} \quad (14)$$

It is observed that, in accordance with the criteria for quasisteady motion, the time derivative of  $\varepsilon_s$  is neglected in the formulation of  $\alpha_s$ , but is retained as a first-order term in the pitch-rate equation. We also note that:

$$\begin{cases} \alpha(s) = \alpha - s\dot{\theta}/V \\ n_z(s) = n_z + s\dot{\theta}/g \end{cases} \quad (15)$$

The initial condition for the structural angle of attack is obtained from Eq. (14):

$$\alpha_{s0} = \frac{(\alpha_0 - d_0 - d_4\delta_0 - d_5)}{(1 + d_1)} \quad (16)$$

The combination of Eqs. (8) and (14–16) yields:

$$\Delta\alpha_s = [C_{11}, C_{12}]\mathbf{u} + D_1\Delta\delta \quad (17)$$

where

$$C_{11} = G_{11} + G_{21}A_{11} + G_{22}A_{21}$$

$$C_{12} = G_{12} + G_{21}A_{12} + G_{22}A_{22}$$

$$D_1 = G_{21}B_1 + G_{22}B_2 - \frac{d_4}{(1 + d_1)}$$

$$G_{11} = \frac{1}{(1 + d_1)}$$

$$G_{12} = \frac{-\tau(d_3 + d_5\nu + \sigma)}{(1 + d_1)}$$

$$G_{21} = \frac{\tau(d_5\nu - d_2)}{(1 + d_1)}$$

$$G_{22} = \frac{-\tau^2(d_5\sigma\nu + d_6 - d_2\sigma)}{(1 + d_1)}$$

For derivation of the sensor pitch rate we differentiate Eq. (9). Combination with Eqs. (14–16) yields

$$\dot{\varepsilon}_s = [G_{31}, G_{32}](A\mathbf{u} + B\Delta\delta) + D_1\dot{\delta} \quad (18)$$

where

$$G_{31} = C_{11} - 1$$

$$G_{32} = C_{12} + \tau\sigma$$

Eliminating the unsteady  $\dot{\delta}$  term and substituting Eq. (18) into Eq. (11) we obtain

$$\dot{\theta}_s = [C_{21}, C_{22}]\mathbf{u} + D_2\Delta\delta \quad (19)$$

where

$$C_{21} = G_{31}A_{11} + G_{32}A_{21}$$

$$C_{22} = 1 + G_{31}A_{12} + G_{32}A_{22}$$

$$D_2 = G_{31}B_1 + G_{32}B_2$$

By defining an output vector

$$\mathbf{u}_s = \begin{Bmatrix} \Delta\alpha_s \\ \dot{\theta}_s \end{Bmatrix} \quad (20)$$

the sensor equations may be expressed in the following condensed form:

$$\mathbf{u}_s = C\mathbf{u} + D\Delta\delta \quad (21)$$

The elements of matrices  $C$  and  $D$  are defined in connection with Eqs. (17) and (19).

### Evaluation of Method

The vehicle response equations [Eqs. (8) and (21)], were programmed using the Matrix<sub>X</sub> software package.<sup>5</sup> One concern was the apparent singularity (for  $d_1 = -1$ ) in Eqs. (16) and (17). This difficulty, which was found to occur for the B-2 aircraft at high dynamic pressure, is caused by numerical truncation in the vicinity of a 0/0 type limit. In the simulation the problem was solved by a procedure that bypasses the narrow range of dynamic pressure for which numerator and denominator terms in the output equation [Eq. (21)] are close to zero. It is important to note that this equation must be based on a consistent set of aerodynamic and aeroelastic coefficients. Since the  $d$  coefficients of Eq. (12) are determined analytically, the output equations require similarly computed aerodynamic data. This requirement, which does not apply to the aerodynamics of the basic equation [Eq. (8)], becomes

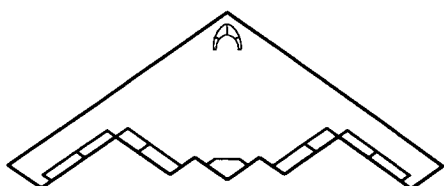


Fig. 3 B-2 planform.

more important as the dynamic pressure increases and the angle between the axes widens.

Evaluations of the new methodology were based on a simple beam idealization of the B-2 as represented by 179 DOFs for the structure and 384 control points for the aerodynamic vortex-lattice model. An outline of the B-2 planform is shown in Fig. 3. To achieve a true comparison between the original equations and the present formulation, a theoretical database

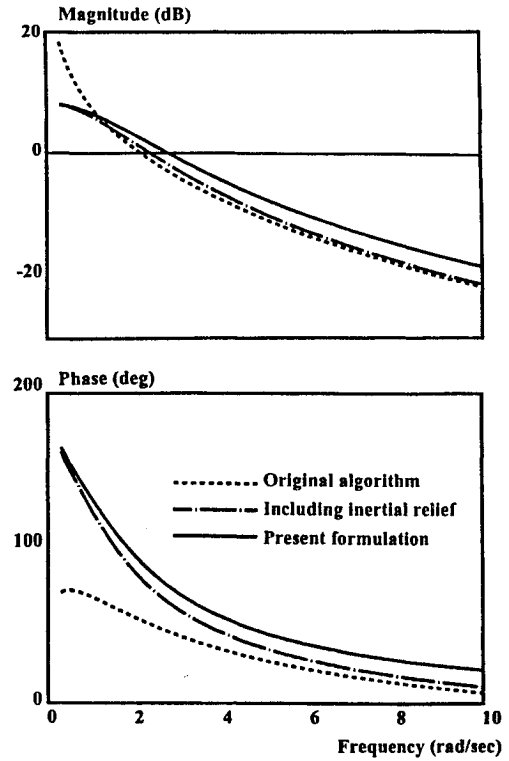


Fig. 4 Theoretical angle-of-attack response.

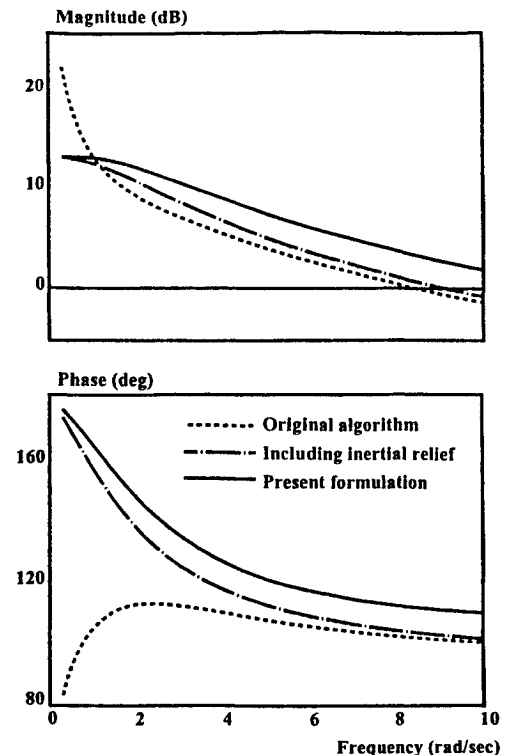


Fig. 5 Theoretical pitch rate response.

was developed by applying the MSC/Nastran aeroelastic analysis code.<sup>6</sup> Transfer functions derived from the two formulations are shown in Figs. 4 and 5 for sensor responses due to pitch control input. The differences are significant. It should be noted, however, that the original algorithm in this evaluation neglected all inertial relief terms as well as the relative motion of the sensor axis. Inertial relief due to translational acceleration, for instance, accounts for the gravitational (1 g) load deformations of the structure. In the chosen example the elimination of these terms produces a statically unstable response. The effect of sensor axis rotation was isolated to demonstrate that it is an important component of the B-2 maneuver response. This evaluation, which also is presented in Figs. 4 and 5, was performed by adding all the inertial relief terms to the original equations and comparing the results with data derived from the current formulation.

### Correlation with Flight Test Data

During the flight test program, the vehicle response due to pilot commands was telemetered to a ground station and re-

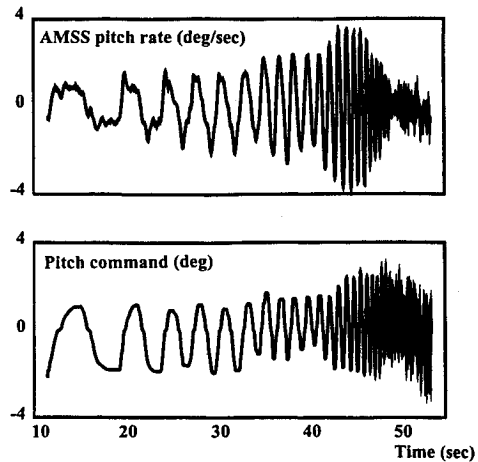


Fig. 6 Time history of pilot command and resulting pitch rate.

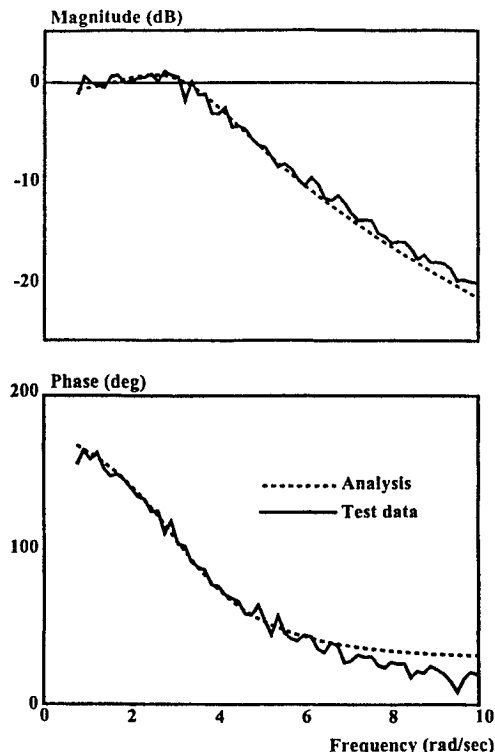


Fig. 7 B-2 angle-of-attack transfer function.

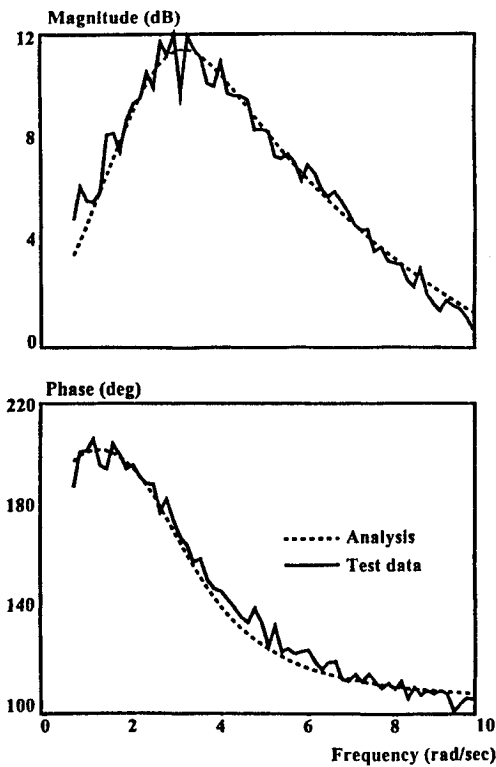


Fig. 8 B-2 pitch rate transfer function.

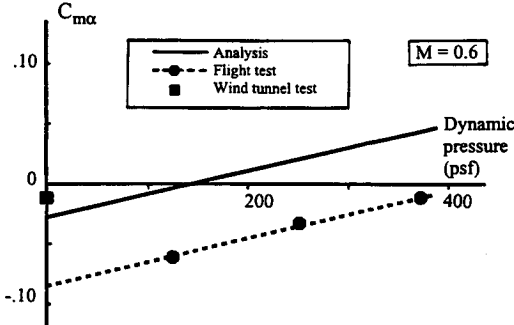


Fig. 9 Aerodynamic pitch moment derivative.

corded on the computerized test data system. A representative time history of the pilot input and the resulting pitch rate are illustrated in Fig. 6. The open-loop transfer functions for various motion variables were generated by computing the ratios between the cross-power spectra and the autopower spectrum for the control excitation. Typical results are shown in Figs. 7 and 8 for the angle of attack and the pitch rate measurements supplied by the attitude/motion sensor set (AMSS), which is located near the pilot station. At the chosen flight condition, the inboard and the midspan elevons are used for pitch control.

Before addressing the correlation between test and analysis, a summary discussion of the aerodynamic database is required. Quasisteady flight tests (i.e., wind-up turns) have shown that the aircraft is statically more stable and has lower pitch damping than indicated by wind-tunnel tests and preliminary analyses. Thus, in the equations of motion the moment derivatives  $C_{m\alpha}$  and  $(C_{m\alpha} + C_{m\beta})$  need to be adjusted to produce short period characteristics (frequency and damping) that match the test data. Confirming results of the quasisteady flight test, a graph of  $C_{m\alpha}$  derived from estimates of the short period frequency is presented in Fig. 9. The corresponding analytical data, although offset from the test results, indicate that aeroelastic effects (as measured by the slope of the graph) are

**Table 1 Sources of aerodynamic data**

Derivative	Source
$C_{za}$ , $C_{zb}$ , $C_{mb}$	Wind tunnel
$C_{ma}$ , $C_{mb}$	Flight test
$C_{zq}$ , $C_{za}$ , $C_{mq}$	Analysis

predicted correctly. The wind-tunnel measurement is plotted on the axis for zero dynamic pressure since aeroelastic deflections of the model are negligible. It is close to the analytical value for the undeformed vehicle.

Analytical results presented in Figs. 7 and 8 were obtained by using aerodynamic data from a combination of wind-tunnel measurement, flight test, and analysis. The source of each derivative is identified in Table 1. By a method similar to the one used for  $C_{ma}$ , the term  $(C_{ma} + C_{mq})$  was computed from an estimate of the damping in the short period mode. Coefficients derived from wind-tunnel measurements were combined with analytical factors (elastic/rigid ratios) that account for aeroelastic effects. These factors and other aeroelastic terms were generated in the MSC/Nastran code by using a more detailed airframe model than the one described in the preceding section. While retaining the aerodynamic lattice from the preliminary analyses, the structural representation was expanded to 19,300 unconstrained DOFs, 492 of which were employed in the solution process.

### Concluding Remarks

Equations that account for sensor motions relative to the mean inertia axes were derived and applied to the USAF/Northrop B-2 aircraft. Parameters of the equations were generated by employing the MSC-Nastran aeroelastic analysis code.

An evaluation of the methodology led to the conclusion that the output equations must be derived from a consistent (i.e., analytical) database, but that various parameters in the equations of motion may be adjusted to match wind-tunnel measurements or data derived from flight tests. Thus, terms related to  $\dot{\alpha}$  were included in the equations of motion, but were omitted from the output equations since the aeroelastic analysis code did not have the capability to compute load

distributions due to this motion variable. The effect of these derivatives, which may not always be small, was left for future investigation.

Maneuver response analyses that account for the relative sensor motion were compared to early simulation results and then to flight test data. It was demonstrated that the sensor axis rotation is an important component of the aeroelastic vehicle response. Correlation with frequency sweep data confirmed other flight test observations that showed the aircraft to be more stable and less damped in pitch than predicted. After adjustment of the static stability and pitch damping terms, the analytical model produced good agreement with test results.

### Acknowledgments

The authors wish to thank R. F. Ringland, Manager of B-2 Flying Qualities Evaluation, and D. F. Kesler, Northrop Consultant, for helpful discussions and assistance on the analytical simulation. Special recognition is due A. Matarazzo, Principal Engineer in the B-2 Aerodynamics Department, who supplied the aerodynamic test data. We also wish to express our appreciation to R. R. Tye who, as manager of Dynamics, Loads and Mass Properties, provided continuous support for the project.

### References

- <sup>1</sup>Rodden, W. P., and Love, J. R., "Equations of Motion of a Quasisteady Flight Vehicle Utilizing Restrained Static Aeroelastic Characteristics," *Journal of Aircraft*, Vol. 22, No. 9, 1985, pp. 802-809.
- <sup>2</sup>Anon., "An Analysis of Methods for Predicting the Stability Characteristics of an Elastic Airplane—Summary Report," NASA CR-73277, Nov. 1968.
- <sup>3</sup>Dusto, A. R., Brune, G. W., Dornfeld, G. M., Mercer, J. E., Pilet, S. C., Rubbert, P. E., Schwanz, R. C., Smutny, P., Tinoco, E. N., and Weber, J. A., "A Method for Predicting the Stability Derivatives of an Elastic Airplane, Volume I—FLEXSTAB Theoretical Description," NASA CR-114712, Oct. 1974.
- <sup>4</sup>Etkin, B., *Dynamics of Flight*, Wiley, New York, 1959, Chap. IV.
- <sup>5</sup>Anon., "MATRIX<sub>x</sub> System Identification Module User's Guide," Integrated Systems Inc., MDG 010-042, Santa Clara, CA, April 1992.
- <sup>6</sup>Rodden, W. P. (ed.), "MSC/NASTRAN Handbook for Aeroelastic Analysis," The MacNeal-Schwendler Corp., MSR-57, Los Angeles, CA, Nov. 1987.